European Journal of Pharmaceutical Sciences

Identification of novel inhibitors of rat Mrp3.

--Manuscript Draft--

Manuscript Number:	PHASCI-D-20-01958R1
Article Type:	Research Paper
Keywords:	Rat hepatocytes; Inside-out membrane vesicles; Multidrug Resistance associated Protein-3 (Mrp3); 5(6)-Carboxy-2′,7′-dichlorofluorescein diacetate; Inhibitor screening; Naive Bayesian model; Computational modeling
Corresponding Author:	Pieter Annaert, PhD KU Leuven Leuven, BELGIUM
First Author:	Tom De Vocht
Order of Authors:	Tom De Vocht
	Christophe Buyck
	Neel Deferm
	Bing Qi
	Pieter Van Brantegem
	Herman van Vlijmen
	Jan Snoeys
	Eef Hoeben
	An Vermeulen
	Pieter Annaert
Manuscript Region of Origin:	BELGIUM
Abstract:	Multidrug resistance-associated protein (MRP; ABCC gene family) mediated efflux transport plays an important role in the systemic and tissue exposure profiles of many drugs and their metabolites, and also of endogenous compounds like bile acids and bilirubin conjugates. However, potent and isoform-selective inhibitors of the MRP subfamily are currently lacking. Therefore, the purpose of the present work was to identify novel rat Mrp3 inhibitors. Using 5(6)-carboxy-2',7'-dichlorofluorescein diacetate (CDFDA) as a model-(pro)substrate for Mrp3 in an oil-spin assay with primary rat hepatocytes, the extent of inhibition of CDF efflux was determined for 1584 compounds, yielding 59 hits (excluding the reference inhibitor) that were identified as new Mrp3 inhibitors. A naive Bayesian prediction model was constructed in Pipeline Pilot to elucidate physicochemical and structural features of compounds causing Mrp3 inhibition. The final Bayesian model generated common physicochemical properties of Mrp3 inhibitors. For instance, more than half of the hits contain a phenolic structure. The identified compounds have an AlogP between 2 and 4.5, between 5 to 8 hydrogen bond acceptor atoms, a molecular weight between 260 and 400, and 2 or more aromatic rings. Compared to the depleted dataset (i.e. 90% remaining compounds), the Mrp3 hit rate in the enriched set was 7.5-fold higher (i.e. 17.2% versus 2.3%). Several hits from this first screening approach were confirmed in an additional study using Mrp3 transfected inside-out membrane vesicles.

Identification of novel inhibitors of rat Mrp3

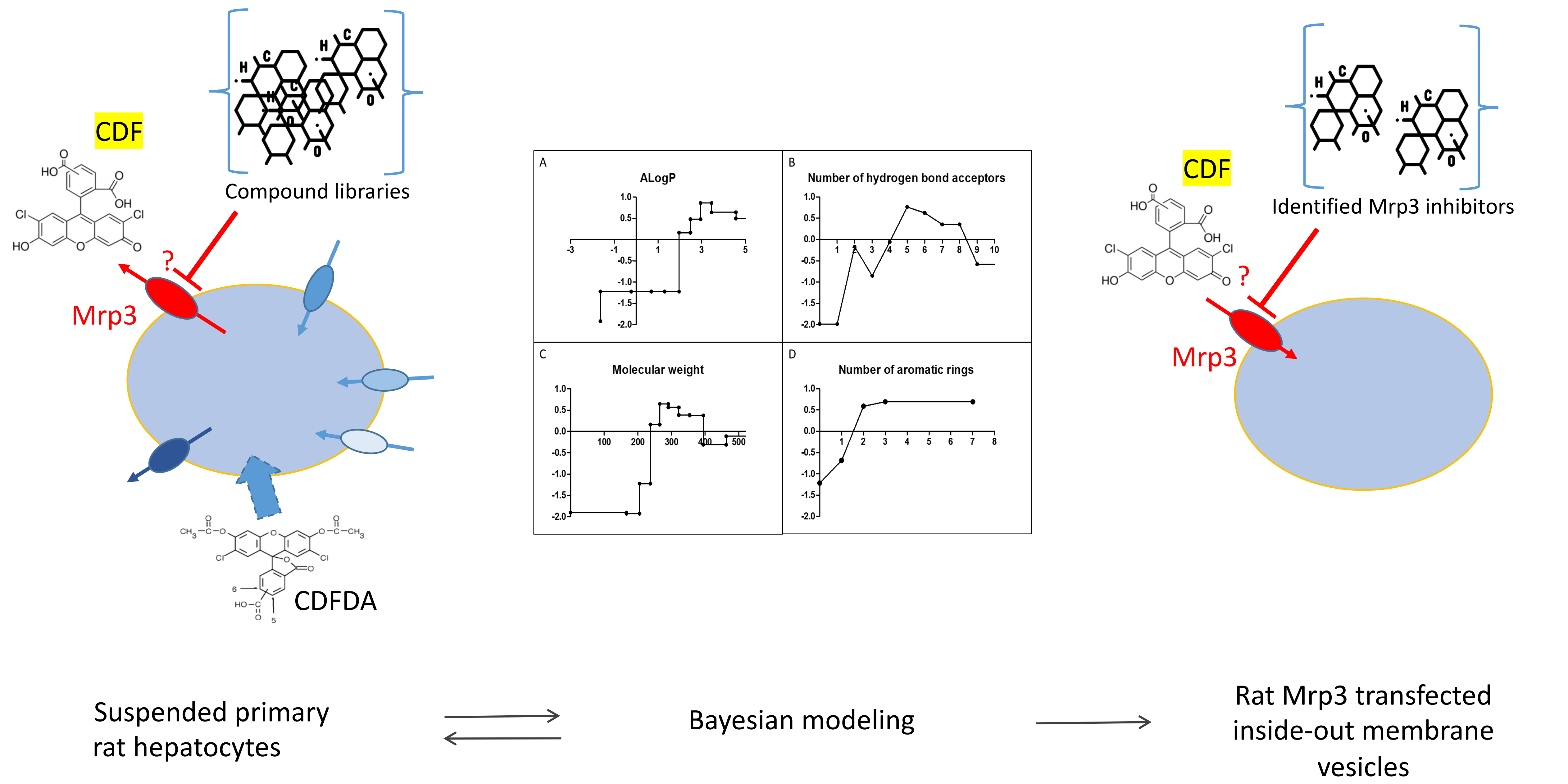

Title page:

Identification of novel inhibitors of rat Mrp3.

Tom De Vocht[1], Christophe Buyck[2], Neel Deferm[1], Bing Qi[1], Pieter Van Brantegem[1], Herman van Vlijmen[2], Jan Snoeys[3] , Eef Hoeben[4, 5], An Vermeulen[4] and Pieter Annaert[1, 5]*

[1]Laboratory of Drug Delivery and Disposition, KU Leuven Department of Pharmaceutical and Pharmacological Sciences, Campus Gasthuisberg, O&N 2, Herestraat 49 box 921, B-3000 Leuven, Belgium.

[2]Discovery Sciences, Janssen Research & Development, a division of Janssen Pharmaceutica N.V., Turnhoutseweg 30, B-2340 Beerse, Belgium

[3]Drug Metabolism and Pharmacokinetics, Janssen Research & Development, a division of Janssen Pharmaceutica N.V., Turnhoutseweg 30, B-2340 Beerse, Belgium

[4]Quantitative Sciences, Janssen Research and Development, a division of Janssen Pharmaceutica N.V., Turnhoutseweg 30, B-2340 Beerse, Belgium

[5]BioNotus GCV, Wetenschapspark Universiteit Antwerpen, Galileilaan 15, B-2845 Niel, Belgium

Running title page:

Running title: Identification of novel Mrp3 inhibitors

*** Corresponding author:**

Pieter Annaert

Laboratory of Drug Delivery and Disposition

KU Leuven Department of Pharmaceutical and Pharmacological Sciences

Campus Gasthuisberg, O&N 2, Herestraat 49 box 921, B-3000 Leuven, Belgium

Tel: +32-16-330303

Email: pieter.annaert@kuleuven.be

Number of text pages: 27

Number of tables: 0

Number of figures: 7

Number of references: 39

Number of words in abstract: 258

Number of words in introduction: 688

Number of words in discussion: 1404

List of nonstandard abbreviations:

AUC	Area under the curve
CDF	5(6)-carboxy-2’,7’-dichlorofluorescein
CDFDA	5(6)-carboxy-2',7'-dichlorofluorescein diacetate
DDI	Drug-drug interaction
DMEM	Dulbecco’s modified Eagle’s medium
DMSO	Dimethyl sulfoxide
FBS	Fetal bovine serum
FCFP	Functional circular fingerprints
KHB	Krebs Henseleit buffer
LLOQ	Lower limit of quantification
MRP	Multidrug resistance-associated protein
OATP	Organic anion transporting polypeptide
PBPK	Physiologically based pharmacokinetics
PBS	Phosphate buffered saline
PK	Pharmacokinetics
RT	Room temperature

Abstract

Multidrug resistance-associated protein (MRP; *ABCC* gene family) mediated efflux transport plays an important role in the systemic and tissue exposure profiles of many drugs and their metabolites, and also of endogenous compounds like bile acids and bilirubin conjugates. However, potent and isoform-selective inhibitors of the MRP subfamily are currently lacking. Therefore, the purpose of the present work was to identify novel rat Mrp3 inhibitors. Using 5(6)-carboxy-2',7'-dichlorofluorescein diacetate (CDFDA) as a model-(pro)substrate for Mrp3 in an oil-spin assay with primary rat hepatocytes, the extent of inhibition of CDF efflux was determined for 1584 compounds, yielding 59 hits (excluding the reference inhibitor) that were identified as new Mrp3 inhibitors. A naive Bayesian prediction model was constructed in Pipeline Pilot to elucidate physicochemical and structural features of compounds causing Mrp3 inhibition. The final Bayesian model generated common physicochemical properties of Mrp3 inhibitors. For instance, more than half of the hits contain a phenolic structure. The identified compounds have an AlogP between 2 and 4.5, between 5 to 8 hydrogen bond acceptor atoms, a molecular weight between 260 and 400, and 2 or more aromatic rings. Compared to the depleted dataset (i.e. 90% remaining compounds), the Mrp3 hit rate in the enriched set was 7.5-fold higher (i.e. 17.2% versus 2.3%). Several hits from this first screening approach were confirmed in an additional study using Mrp3 transfected inside-out membrane vesicles.

In conclusion, several new and potent inhibitors of Mrp3 mediated efflux were identified in an optimized *in vitro* rat hepatocyte assay and confirmed using Mrp3 transfected inside-out membrane vesicles. A final naive Bayesian model was developed in an iterative way to reveal common physicochemical and structural features for Mrp3 inhibitors. The final Bayesian model will enable *in silico* screening of larger libraries and *in vitro* identification of more potent Mrp3 inhibitors.

Keywords:

Rat hepatocytes, Inside-out membrane vesicles, Mrp3, Efflux transporter, 5(6)-Carboxy-2′,7′-dichlorofluorescein diacetate, Inhibitor screening, Naive Bayesian model, Computational modeling

Introduction

Over the past decade, the role of transporters in pharmacokinetic (PK) processes and drug-drug interactions (DDIs) has been increasingly recognized (International Transporter Consortium et al., 2010). The growing concern about the impact of drug-drug, drug-endogenous/exogenous metabolites, drug-toxin, drug-nutrient and toxin-metabolite interactions in a clinical setting has been driving this expanded interest in drug transporters. These compounds can potentially compete with one another for binding to the same transporter, thereby leading to unexpected changes in plasma/serum and tissue drug levels, possibly resulting in unwanted side effects (Nigam, 2015). This also implies that, during drug development, it is very important to determine the affinity and/or inhibitory effects of drug candidates for drug transporters. Regarding DDIs at the level of uptake of compounds in the liver, a lot of research has been done with e.g. statins (De Bruyn et al., 2013; Kalliokoski and Niemi, 2009; Maeda, 2015; Parvez et al., 2016). In contrast, knowledge of DDIs at the level of sinusoidal efflux of compounds from the hepatocytes back to the blood compartment remains scarce. Because of their pivotal role in hepatic sinusoidal efflux, several MRP isoforms (MRP3, MRP4 and MRP5) are of particular interest. These transporters are known to transport endogenous and xenobiotic anionic substances relying on ATP as energy source. Also, prior nonclinical and clinical research illustrates that MRP-mediated efflux of many drugs, their metabolites, and endogenous compounds such as bile acids, plays an important role in the systemic and tissue exposure profiles of these compounds (Fukuda et al., 2013; Shao et al., 2014). Examples of drugs and endogenous compounds influenced by MRPs in terms of absorption, distribution and/or excretion are bile acids, fexofenadine, diclofenac-acyl-glucuronide and methotrexate (Hirohashi et al., 2000; Kawase et al., 2016; Matsushima et al., 2008; Scialis et al., 2015). Recent findings have also suggested that MRPs play an important pathophysiological role in the multidrug resistance effect of several cancers and other diseases such as cholestasis (Rodrigues et al., 2014; Zhang et al., 2015). Another example showing the importance of the MRP transporter is the modulation of its function by inhibitors to re-sensitize chemotherapeutic agents in cancer therapy

(Zhang et al., 2015). A problem to investigate MRPs in general is the limited availability of potent isoform-selective MRP inhibitors (Köck and Brouwer, 2012). Examples of compounds known to inhibit multiple MRP transporters are MK571 and benzbromarone (Ali et al., 2017; Gilibili et al., 2017). 5(6)-carboxy-2',7'-dichlorofluorescein (CDF) is a well characterized fluorescent substrate of the (rat) Mrp3 efflux transporter and other Mrp transporters (Fardel et al., 2015). In rat hepatocytes and isolated perfused rat liver, CDF was shown to be transported via Mrp2 into the bile and via Mrp3 into the sinusoidal blood, after which it can undergo cellular re-uptake via Oatp-mediated transport (Zamek-Gliszczynski et al., 2003). Mrp2 was shown to carry out the majority of CDF efflux, while the role of Mrp3 was shown to increase in the absence of Mrp2 (Ellis et al., 2014). During cholestasis, a disorder which is characterized by the pathological accumulation of bile salts, the basolateral MRP3 and MRP4 efflux transporters are induced, resulting in diminished intracellular levels of biliary constituents (Deferm et al., 2019). In summary, we present the development of an *in vivo* relevant *in vitro* assay that can be used to evaluate the Mrp3 inhibitory potential of compounds. Using fluorescence spectroscopy, we quantified the inhibitory effect of a structurally diverse set of 1584 test compounds on Mrp3 in suspended rat hepatocytes by calculating the relative inhibitory effect of these molecules compared to that of the well-known Mrp inhibitor benzbromarone (Jemnitz et al., 2010). An additional study with part of the hits was done as confirmation using Mrp3 transfected inside-out membrane vesicles. By using our results in an iterative way as an input, a Bayesian predictive model was constructed. This model allows to screen other libraries more efficiently which will facilitate synthesis of more specific Mrp3 inhibitors in the future. Also, chemical features shared by compounds that are active as opposed to chemical features shared by inactive compounds were documented. This can be a first step towards a similar assay using human suspended hepatocytes to investigate inhibition of human MRP3.

Materials and methods

Materials

Darunavir ethanolate, tipranavir, ritonavir, atazanavir sulfate, and amprenavir were provided by the National Institutes of Health AIDS Research and Reference Reagent Program (Germantown, MD). Saquinavir mesylate, indinavir sulfate, nelfinavir mesylate, and lopinavir were donated by Hetero Drugs Ltd. (Hyderabad, India). Dulbecco's modified Eagle's medium (DMEM), L-glutamine, penicillin-streptomycin (10.000 IU/mL, 10.000 µg/mL), and phosphate buffered saline (PBS) were purchased from Westburg (Leusden, The Netherlands). HEPES (4-(2-hydroxyethyl)-1-piperazineethanesulfonic acid) was purchased from MP Biochemical (Illkirch, France). Collagenase (Type IV), dexamethasone, Triton X-100, benzbromarone, insulin from human origin, mineral oil, silicon oil, 5(6)-Carboxy-2',7'-dichlorofluorescein diacetate (CDFDA), 5(6)-Carboxy-2',7'-dichlorofluorescein (CDF) and Percoll™ were purchased from Sigma-Aldrich (Schnelldorf, Germany). Sodium chloride (NaCl) was obtained from Fisher Chemical (Landsmeer, The Netherlands), potassium chloride (KCl) from AppliChem (Darmstadt, Germany), magnesium chloride ($MgCl_2$) from Analar-Normapur (VWR) (Leicestershire, UK), glucose from Fisher Scientific (Erembodegem, Belgium), calcium chloride ($CaCl_2$) and sodium hydrogen carbonate ($NaHCO_3$) were obtained from Chem-Lab NV (Zedelgem, Belgium). Synth-a-Freeze™ was purchased from Life Technologies (Gent, Belgium). Fetal bovine serum (FBS), Trypan blue stain (0.4%) and 10x phosphate buffered saline (PBS) were obtained from Lonza SPRL (Verviers, Belgium). The transport buffer, wash buffer, ATP mix and rat Mrp3-expressing inside-out membrane vesicles (protein concentration 5 mg/mL) derived from HEK-293 cells were provided by Solvo Biotechnology (Szeged, Hungary). The Spectrum Collection (2000 compounds, supplied as 10mM DMSO solution) was purchased from MicroSource Discovery Systems Inc. (Gaylordsville, CT). A selection of compounds of the Janssen corporate compound collection (140 compounds, supplied as 5 mM DMSO solution) were kindly offered by Janssen Research & Development, a division of Janssen Pharmaceutica N.V. (Beerse, Belgium).

Methods

Animals

Male Wistar rats in the weight range of 180 – 220 g (Janvier, France) were used for isolation of hepatocytes. The animals were housed according to the Belgian and European laws, guidelines and policies for animal experiments, animal housing and animal care in the Central Animal Facility of the KU Leuven. Approval for the experiments was granted by the Institutional Ethical Committee for Animal Experimentation of the KU Leuven (license number: P014/2015).

Isolation and cryopreservation of rat hepatocytes

Rat hepatocytes were isolated using a 2-step collagenase perfusion (Annaert et al., 2001). After isolation, cells were centrifuged at 50*g* for 3 min at 4°C and the pellet was resuspended in Synth-a-Freeze™. Hepatocytes were cryopreserved in vials containing 10 million viable cells/ml using a controlled freezing program with Planer Kryo 560-16 machine (SolutionsCryo, 's Hertogenbosch, The Netherlands). Afterwards, the vials were stored in liquid nitrogen.

Thawing of cryopreserved rat hepatocytes

Immediately before efflux experiments, cryopreserved hepatocytes from male Wistar rats were rapidly thawed by gently shaking the vial in a 37°C water bath. As soon as all ice crystals were melted, the content was transferred to a 50 mL polypropylene tube containing a thawing mixture of 25 mL thawing medium (DMEM supplemented with 10% FBS (v/v), 2 mM L-glutamine, 1 µM dexamethasone, 4 µg/mL insulin, 100 IU/mL penicillin, 100 µg/mL streptomycin) and 16 mL isotonic Percoll™ solution (90% Percoll™, 10% 10x concentrated PBS) at 37°C. Cryogenic vials were rinsed twice with thawing mixture before the 50mL tubes were centrifuged (168*g*) for 20 min at room temperature (RT). After removing the supernatant, the pellet was re-suspended in 20 mL of thawing mixture and again centrifuged (50*g*) for 3 min at RT. After removing the supernatant a second time, rat hepatocytes were re-suspended in Krebs Henseleit buffer (KHB) (NaCl 130 mM, KCl 5.17 mM, $CaCl_2$ 1.2 mM, $MgCl_2$ 1.2 mM, HEPES 12.5 mM, glucose 11.1 mM, Na-pyruvate 5 mM; pH 7.4) which had been sparged with carbogen (95%/5% O_2/CO_2) for 10 min. Cell viability and cell density of hepatocytes were evaluated using the Trypan blue (0.04%) exclusion method. Cell viability was always higher than 70%.

In vitro screening of libraries to identify novel Mrp3 inhibitors

A graphical representation of the optimized assay used to screen for Mrp3 inhibitors in rat hepatocytes in suspension is shown in Figure 1. After the thawing procedure, cells were diluted with KHB to a four-fold concentrated cell density (4 million cells/mL). Two-fold concentrated CDFDA (10 µM) solutions and four-fold concentrated benzbromarone (20 µM) or test compound solutions (60 µM) were prepared in KHB (< 0.5% final DMSO content). These optimal concentrations were determined in concentration dependent CDF efflux experiments (Supplemental Figures 2 and 3). Efflux studies were performed using the oil-spin method (Nicolaï et al., 2017). Hepatocytes (175 µL) were pre-incubated for 10 min at 37°C. Following pre-incubation, benzbromarone (reference inhibitor) or the test compound (175 µL) was added together with CDFDA (350 µL) and the efflux of CDF was assessed. Immediately after 3 and 5 minutes incubation time, the optimal time points determined in time dependent CDF efflux experiments (Supplemental Figure 1), triplicate 200 µL aliquots were rapidly pipetted on top of an oil layer (82:18 v/v silicon oil:mineral oil, 1.051 g/mL) above a NaCl solution (8% w/v) in 1.5 mL test tubes. The test tubes were centrifuged immediately (14462*g*) for 3 min at RT. Without delay, the tubes were snap-frozen in a mixture of dry ice and ethanol (-80°C). After all tubes were frozen, the tube-pellets were collected in glass test tubes by cutting the bottom part (~ 80 µL) with a tube cutter. Pellets were lysed with 300 µL lysis buffer (0.5 % Triton X-100 in PBS), shaken for 40 min (300 rpm, RT, protected from light) on a shake incubator (Ika labortechnik KS125 basic). Following lysis, 200 µL of cell lysates were analyzed by fluorescence spectroscopy (ex 503 nm, em 537 nm) in a Tecan Infinite 200M plate reader (Tecan Benelux, Mechelen, Belgium). In order to determine the inhibiting effect of a test compound on active Mrp3 efflux transporter kinetics, the effect of the test compound on intracellular CDF was measured in triplicate at 3- and 5-min incubation time points. Finally, the remaining amount of intracellular CDF was compared to the remaining intracellular CDF in the presence of benzbromarone (20 µM), which was used as the positive control.

IC_{50} determination of tipranavir

As tipranavir was the most potent compound after screening, we have chosen this for further IC_{50} determination. After the thawing procedure, cells were diluted to a four-fold concentrated cell density (4 million cells/mL). Two-fold concentrated CDFDA (10 µM) solutions and four-fold concentrated tipranavir solutions (0.4 µM, 4 µM, 8 µM, 20 µM, 40 µM, 60 µM, 200 µM) were prepared in KHB (< 0.5% final DMSO content). IC_{50} determination of Mrp3-mediated CDF transport was performed using the oil-spin method as described before (Nicolaï et al., 2017). In order to determine the inhibiting effect, co-incubation of different concentrations of tipranavir on active Mrp3 efflux transporter kinetics was assessed, and intracellular CDF was measured in triplicate at the 3 min incubation time point.

Bayesian model analysis

Naive Bayesian models were generated in the Pipeline Pilot software (Biova Pipeline Pilot v.9.2) to guide compound selection and gather insights on the factors that are important for Mrp3 inhibition. The structures of the compounds were standardized by protonating acids, deprotonating bases and generating the canonical smiles of the compounds using Pipeline Pilot (Weininger, 1988). A set of descriptors that are known to be performant when used for predicting chemically diverse structures were selected as input. These descriptors were divided into physicochemical descriptors (AlogP, molecular weight, number of hydrogen donors, number of hydrogen acceptors, number of aromatic rings, number of rotatable bonds, molecular fractional polar surface area) and a chemical structure descriptor (FCFP_6: Functional Circular FingerPrints of 6 bonds diameters). This means that for the physicochemical descriptors, the default set of parameters was kept. For the fingerprint parameter, the length was reduced from the default twelve to six because reducing the length to 6 makes the model 'forget' the exact input molecules. The Pipeline Pilot component was set up to 'Save Training Properties'. By setting this flag, the training set used for training the model is also saved in an encrypted form as part of the model and by doing so the Tanimoto distances of any given test compound to the closest members used is stored into the component and the distances of a test compound to closest members used in the training set of the model can be generated. Also, the 'Validate Models' option was enabled to store the model performance info based on the Leave-one-out cross validation method. Another option that was enabled is the 'Remove Uninformative Bins', which will eliminate features from the model that do not contribute a lot to the model; all features with less than 0.05 contribution to the model are removed this way. A last parameter that was enabled is the 'Equipopulate Bins': this is used for continuous properties (not for fingerprints) to size the bins into approximately equal number of samples (in this work 10 bins were used). As a result, the bins do not have the exact same width, but the statistical robustness of some otherwise poorly populated bins improves as the number of data points in these bins will be used for creating the boundaries (hence ensuring an optimal distribution over all bins).

Effect of potential modulators on Mrp3 mediated CDF uptake in Mrp3 transfected inside-out membrane vesicles

To examine the inhibition of modulators in another *in vitro* setup, previously determined Mrp3 inhibitors were tested. Mrp3-mediated CDF uptake was determined in Mrp3 transfected inside-out membrane vesicles. 10 µL of ice-cold vesicle-CDF (5 µM) mixture (optimal concentration based on concentration dependent experiments) and 10 µL of inhibitor (15 µM) mix were added to the wells of a V-shaped well plate. Benzbromarone was used as reference inhibitor. Subsequently, 10 µL transport buffer was pipetted into the AMP control wells and the plate was preincubated for 15 minutes at 37°C in a shaker. 10 µL of ATP mixture was then added to the ATP wells and incubated for 30 minutes (optimal incubation time based on time dependent experiments) at 37°C in a plate shaking incubator (250 rpm). To put the ongoing reaction to a halt, 200 µL of ice-cold transport buffer was added. The mixture was washed five times with transport buffer, after transferring the content into a prewetted filter plate. The filter plate was then dried using a Multiscreen$_{HTS}$-Vacuum Manifold filtration device (Merck Millipore) and afterwards a black well plate was placed into the device. Then, the content of the filter plate was lysed with 100 µL of 1N NaOH for 10 minutes and transferred into the black well plate using the vacuum device. Fluorescent intensity was measured by Tecan Infinite 200M plate reader at ex/em wavelength of 503/537 nm. IC_{50} determination of Mrp3-mediated CDF transport was performed. In order to determine the inhibiting effect, co-incubation of different concentrations of tipranavir on active Mrp3 efflux transporter kinetics was assessed, and intravesicular CDF was measured in triplicate.

Data analysis

Fluorescence intensities were corrected for blank (mixture of 4 parts 0.5% Triton X-100 in PBS and 1 part of 8% (w/v) NaCl solution) and corresponding concentrations of CDF in lysate were calculated (MS Excel version 2013) based on a calibration curve ($R^2 \geq 0.995$; 11 data points serially diluted starting from 800 nM CDF, LLOQ of 0.78 nM). Based on the calibration curve, the mean of triplicate measurements was converted to an amount in the cell lysate expressed in pmol/million cells in the lysate.

Screening for Mrp3 inhibitors: The area under the curve between 3 and 5 min incubation time points ($AUC_{3\text{-}5min}$) was calculated using GraphPad Prism® 5.00 software. The percentage of efflux transport inhibition compared to benzbromarone was calculated by applying the following equation:

Equation 1:

$$Relative\ inhibition\ test\ compound\ (\%) = \frac{AUC\ test - AUC\ control}{AUC\ benzbromarone - AUC\ control}\ x\ 100\%$$

IC_{50}: The IC_{50} value of tipranavir was calculated by non-linear regression with least squares fit based on the following equations (Fifty= (Top+Baseline)/2) and (Y= Bottom + (((Top-Bottom)* X) / (X + IC50)))) using GraphPad Prism® 5.00 software.

Results

An iterative approach of screening libraries to identify new Mrp3 inhibitors using *in vitro* measurements and *in silico* modeling

Firstly, to identify new Mrp3 inhibitors in suspended hepatocytes, the existing oil-spin assay needed to be optimized. Based on time- and concentration dependent experiments (Supplemental data), 3 and 5 minutes incubation time points together with 10µM of CDFDA as probe substrate were selected as optimal conditions for further screening purposes. Based on the 3 and 5 minutes intracellular CDF levels in the lysate, compounds were allocated as being an inhibitor or not. A 50% cut-off was chosen to distinguish between inhibitors (active compounds) and non-inhibitors (inactive compounds). After screening 1430 compounds of The Spectrum Collection library (MicroSource Discovery Systems Inc.) and 14 in-house compounds, a hit rate of 2.1% (30 hits out of 1444 compounds) was observed.

Based on this first screening an exploratory naive Bayesian model was constructed in Pipeline Pilot. Using this primary exploratory model, 50 compounds were selected from the Janssen corporate compound collection (database of more than one million compounds from historical purchases and internally synthesized compounds for which physical samples are still available for screening purposes) as possible Mrp3 inhibitors, based on their chemical structures and the availability of chemical quality measurements with at least 80% purity or higher. An updated Bayesian model, including the previous data and the data of the 50 additional Janssen compounds was constructed. To expand and further validate the scope of the updated Bayesian model, a third selection of 90 screening compounds was made for new Mrp3 inhibitors. This selection was broader in terms of diversity and contained molecules that were more dissimilar to the initial test set. The third and final screening resulted in a hit rate of 15.6% (14 hits out of 90 compounds).

The hit rate of this last screening round is still high but lower than in the previous round. This is not surprising as for this round the selection criteria were modified towards selecting compounds that help expand the borders of the model coverage. In other words, we prioritized compounds on their chemical dissimilarity from the training set. We also manually cherry-picked compounds that had a decent score in the model, and their distance from the training set was higher, or the two closest neighbors in the training set consisted of one active and one inactive.

Overall, we observed a 3.7% hit rate (59 hits out of 1584 compounds) based on the following order of screenings and Bayesian model constructions: Screening 1, Bayesian model, Screening 2, Updated Bayesian model, Screening 3, Final Bayesian model. An overview of all hits with their respective relative inhibition compared to benzbromarone is shown in Figure 2A and listed in Supplementary Table 1. An overview of the screening rounds and the respective hit rates is shown in Figure 2B. After the 3rd and final *in vitro* screening, the final naive Bayesian model was constructed.

IC_{50} determination of tipranavir

Based on the inhibitory potency assay in suspended hepatocytes, an IC_{50} value (mean ± SEM) was calculated for the most potent inhibitor from the different libraries screened. Tipranavir had an IC_{50} of 7.4 ± 2.1μM for Mrp3 mediated transport of CDF (Figure 3). Based on the inhibitory potency assay in membrane vesicles (Figure 4), an IC_{50} value (mean ± SEM) was again calculated for the different inhibitors. Tipranavir had an IC_{50} of 24.9 ± 9.8μM for Mrp3 mediated transport of CDF (Figure 5).

Bayesian model analysis

Physicochemical features associated with Mrp3 inhibition

The four most pronounced physicochemical features discriminating Mrp3 inhibitors and non-inhibitors include lipophilicity, number of hydrogen bond acceptors, molecular weight, and number of aromatic rings (Figure 6).

The lipophilicity of the screened compounds was investigated (panel A). It is clear that lipophilic compounds are preferred for being an Mrp3 inhibitor. Compounds with an AlogP ~ 3 are having the highest normalized probability to be an Mrp3 inhibitor. In panel B, the normalized probability of the number of hydrogen bond acceptors a possible Mrp3 inhibitor contains is illustrated: at least 2 (and optimally 5) hydrogen bond acceptor atoms (O, N, S or P) are more likely to yield an Mrp3 inhibitor. The molecular weight of the screened compounds (panel C) was also an important descriptor to distinguish Mrp3 inhibitors from non-inhibitors. Small fragment-like molecules with molecular weight < 260 Da are less likely to have affinity at the screened concentration, while a molecular weight ~ 300 Da seems to be the optimal for Mrp3 inhibitors. It appears that there is also an upper threshold for molecular weight (<400 Da), above which a decreased chance of finding Mrp3 hits exists. Finally, the number of aromatic rings (panel D) is a parameter that distinguishes the screened Mrp3 inhibitors from the non-inhibitors. Compounds containing two or more aromatic rings had a high normalized probability to be an Mrp3 inhibitor.

All this information allows splitting the dataset based on the physicochemical properties into an enriched and a depleted region. The enriched region isolates about 10% of the compounds. These compounds have an AlogP between 2 and 4.5, between 5 to 8 hydrogen bond acceptor atoms, a molecular weight between 260 and 400 and two or more aromatic rings. The depleted region entails the 90% remaining compounds. Compared to the depleted dataset, the Mrp3 hit rate in the enriched set is 7.5 fold higher (2.3% in the depleted set, 17.2% in the enriched set).

Examples of Mrp3 hits containing these optimal features are shown in Supplemental Table 2.

Structural features associated with Mrp3 inhibition

Mrp3 is known to have an affinity for acidic structures (Kool et al., 1999), hence it is not a surprise that structures containing acidic functionalities are amongst the most discriminating sub-structural features in the model. Phenolic acids are the predominant structural features occurring in hits, since more than half of the hits contain a phenolic structure. Therefore, the Bayesian model uses many phenolic features to identify possible Mrp3 candidates: 15 of the top 20 structural features are phenolic acids, the other 5 substructures originate from molecules with phenolic acids.

There are 316 phenols present in the dataset of which 37 have been identified as Mrp3 inhibitor. The chance of having Mrp3 activity solely based on the presence of a phenolic moiety in the structure is 12% (37 phenolic hits out of 316 phenolic structures). Some examples of hit molecules are shown in Figure 7. Consistent with the idea that a lot of Mrp3 inhibitors are acidic in nature is the finding that sub-structural features that are containing a basic moiety are found in the top scoring discriminating features for inactive molecules. Examples of non-hit molecules are shown in Figure 8.

Screening approach for identification of potential modulators on Mrp3 mediated CDF uptake in Mrp3 transfected inside-out membrane vesicles

To examine the inhibition of Mrp3 mediated CDF uptake in Mrp3 transfected membrane vesicles (Figure 4), time and concentration dependent experiments (Supplementary figures 4 and 5) were conducted to optimize the CDF concentration and incubation time. Out of the hits from the hepatocyte-based screening (Figure 2), 28 compounds including benzbromarone as reference inhibitor were tested in membrane vesicles to determine their inhibitory effect on Mrp3 mediated CDF transport. These 28 compounds were chosen based on the highest inhibitory potential in the previous hepatocyte-based assay study. Using this optimized membrane vesicle assay, a total of 21 out of 28 compounds were confirmed as Mrp3 inhibitor (≥ 50% inhibition compared to reference inhibitor). The comparison between the mean values of uptake ± SD (% of control) and the positive control benzbromarone is shown in Figure 9.

Discussion

The present study aimed to identify novel and potent inhibitors of rat Mrp3 using an optimized and *in vivo*-relevant *in vitro* system in conjunction with a structure-based *in silico* evaluation. An in vitro assay using suspended hepatocytes was developed and was also applied to determine an IC_{50} value of tipranavir, the most potent compound from libraries screened in the present study. An additional study was done with part of the hits for confirmation using Mrp3 transfected membrane vesicles.

Hepatocytes in suspension are known to be 'the gold standard' to investigate the uptake of drugs across the sinusoidal membrane (Bow et al., 2008; De Bruyn et al., 2011; Keemink et al., 2015; Nicolaï, 2015). The big advantage of using suspended hepatocytes over e.g. inside-out membrane vesicles prepared from Mrp-transfected cells, is the *in vivo* relevant expression of the complete spectrum of metabolizing enzymes and transporters. In addition, the viability and function of the hepatocytes remains acceptable for several hours. Also, metabolites can appear in the system itself, which is more relevant for the *in vivo* situation, in contrast to membrane vesicles. Nevertheless, we also used Mrp3 transfected inside-out membrane vesicles to confirm our findings and showed indirectly that our hepatocyte-based assay was indeed probing the Mrp3 transporter. The use of another *in vitro* setup e.g. sandwich-cultured hepatocytes could address an important disadvantage of suspended hepatocytes, which is the loss of polarity and hence less active canalicular efflux transporters (Bow et al., 2008). Nevertheless, the expression of the metabolizing enzymes and transporters in sandwich-cultured hepatocytes is generally less consistent with *in vivo* values. Moreover, the culturing of hepatocytes in sandwich configuration is much more time consuming and labor intensive than using hepatocytes in suspension (Brouwer et al., 2013).

To investigate Mrp3 inhibitors in particular, we were able to use hepatocytes in suspension because only Mrp2 and Mrp3 are expressed at the membrane of rat hepatocytes to an extent that is relevant for drug disposition (Chen et al., 2005; Zhu et al., 2017). Previous literature reports have demonstrated that, based on imaging, Mrp2 internalization occurs extensively when using suspended hepatocytes (Bow et al., 2008; Sekine et al., 2011), supporting exclusive evaluation of the role of Mrp3, i.e. with minimal interference by Mrp2. Furthermore, preliminary experiments elucidated that CDF is a good substrate for rat Mrp2/human MRP2 and rat Mrp3 but not for human MRP3 (Heredi-Szabo et al., 2008; Seelheim et al., 2013). As we observed almost no efflux of CDF in suspended human hepatocytes, internalization of canalicular efflux transporters in suspended hepatocytes appears likely. Consequently, the hits determined with the present approach are assumed to be primarily Mrp3 inhibitors, in view of both the affinity profile of the substrate used, as well as the predominant expression of the Mrp3 isoform at the sinusoidal membrane. In addition, together with the internalization, the remaining canalicular membrane domain in suspended rat hepatocytes accounts for only 10-15% of the total cell membrane area, consistent with a very limited role for Mrp2 in this *in vitro* assay. It would be interesting to have direct evidence by demonstrating Mrp2/Mrp3 localization as a topic of future research, although this was out of scope for the current study. Mrp3 internalization is unlikely to happen as we can show indirect evidence through the results shown in supplemental Figure 1. A clear decrease in intracellular CDF as a function of time was observed in control condition. If Mrp3 would be internalized, this would not be the case and an increase in CDF as a function of time would be observed due to intracellular CDF trapping.

A relative disadvantage of using hepatocytes in suspension is the fact that we cannot conclude whether the parent compound or possible metabolite(s) exert the Mrp3 inhibitory function. Although, by using short incubation time points (3 and 5 min) it is more likely that we investigated the parent compound itself rather than its metabolite(s) because metabolism is assumed to be very limited using such short timeframes. In view of the affinity of CDF for SLC transporters, another potential limitation that has to be taken into account is the possibility of reverse functioning of SLC transporters thus mediating CDF efflux independent of Mrp3 activity. However, this mechanism is considered unlikely for two reasons. First there is currently limited evidence for substantial functioning of SLCs in a reverse manner in efflux assays. Secondly, on top of the established role of Mrp3 in CDF efflux, it seems unlikely that OATP-mediated efflux would be significant as extracellular CDF concentrations are rising quickly, exactly due to Mrp3-mediated efflux in the first place. Indeed, as opposed to the established Mrp3-mediated (ATP driven) efflux of CDF even against a concentration gradient, extracellular CDF concentrations would rapidly result in OATP-mediated uptake (rather than efflux), making significant OATP-mediated efflux unlikely. The dedicated role of OATP(s) and Mrp3 in the sinusoidal uptake and efflux, respectively, of CDF has been shown previously in isolated perfused rat liver experiments (Zamek-Gliszczynski et al., 2003). Because two time points (3 and 5 minutes) were used in the developed assay, an AUC could be calculated which increased the robustness of the assay. Lower concentrations of screened compounds (15 µM) were used as opposed to previous studies (100 µM) (Ali et al., 2017; Gilibili et al., 2017). As a result, only compounds with at least an intermediate potency for inhibition of Mrp3-mediated CDF efflux were obtained, thus increasing the specificity of the assay.

The 50% cutoff between active or inactive compounds was chosen rather arbitrarily but was well considered because we were primarily interested in potent inhibitors being active at a low concentration of 15 µM and therefore having a significant extent of Mrp3 inhibition. Consequently, only these potent Mrp3 inhibitors were finally implemented as hits in the Bayesian model.

The obtained results for physicochemical features important for being an Mrp3 inhibitor are consistent with recent findings for human MRP3 inhibitors (Ali et al., 2017). In the latter study lipophilicity, molecular weight and the number of aromatic rings of the tested compound were also important to distinguish MRP3 inhibitors from non-inhibitors. Based on the knowledge that there is an 83% similarity with human MRP3 at amino acid level (Kiuchi et al., 1998), we conducted an overlap analysis with the compounds used to build the Bayesian model and the ones described in Ali *et al*. Of the 86 compounds previously reported in the Ali *et al* article, 42 were also present in our set of 1584 tested compounds. Because differences in used substrate, assay and applied concentration of the screened compounds, we can expect differences in the results obtained. Considering a cutoff value of 50%, nine compounds of the common 42 were active in the conditions used by Ali *et al*. Only benzbromarone shows activity at the lower concentration we used, not surprisingly the most potent of the 9 active compounds in this compared subset.

Many of the hits contain phenolic acid substructures. If we assume that the molecules having phenolic esters could be metabolized to their corresponding acids, then the fraction of phenolic-like hits could possibly further be increased to >85% of the hits. Some example molecules that could potentially be metabolized to the corresponding phenolic acids are shown in Figure 10.

The tested dataset contains a diverse set of 265 carboxylic acids, but none of them show more than 50% inhibition at the tested concentration. Conversely, sub-structural features containing carboxylic acids are present as top scoring discriminating features for inactive molecules. The impact of membrane permeation on inhibitor potential will also apply for these compounds *in vivo*. In addition, the suspended hepatocytes offer the implicit advantage that also uptake transporters are functional on the sinusoidal membrane. In other words, negatively charged compounds that are actively taken up by other transporters should not have reduced inhibition potential as compared to the *in vivo* situation.

A large number of compounds from two different libraries were screened in an iterative way using computational modeling, which made our Bayesian model more powerful for future purposes. In fact, each screening round was a validation of the previously obtained results. In general, the Bayesian model is a useful tool to prioritize molecules when the screening capacity is limited. Based on prior knowledge gathered from the previously screened molecules, it enables focusing on the regions of the (physico-)chemical space where the probability of finding additional inhibitors is higher (or lower if desired). In addition, since the implementation also keeps track of the original training set, the user is able to see how chemically distant a potential test molecule is from the training set. Additionally, it is important to realize that a Bayesian model is categorical. It separates one group of compounds (Mrp3 active ones with more than 50% inhibition) from another group of compounds (inactive ones, i.e. less than 50% inhibition). As a consequence, 60% inhibition is treated equally to 90% inhibition. The resulting Bayesian score will differentiate molecules based upon this classification but does not automatically reflect how potent a molecule will be. The currently developed Mrp3 Bayesian model, which is included as supplementary material, enables *in silico* screening of other libraries and therefore discovery of additional Mrp3 inhibitors. An additional study was done as confirmation using Mrp3 transfected inside out membrane vesicles as *in vitro* system. Seventy five % of the hits in the hepatocyte-based assay were confirmed in the vesicle-based assay, showing the resemblance between both *in vitro* screening approaches. This also indirectly indicated that inhibition of Mrp3 was the major transporter-mediated process evaluated in the suspended hepatocytes. In both screening approaches the *in vitro* potency of the most potent Mrp3 inhibitor was determined using the developed assay. The most potent compound out of the different libraries screened using suspended hepatocytes was tipranavir which had an IC_{50} value of 7.4 ± 2.1µM. Using the second screening assay with Mrp3 transfected inside out membrane vesicles tipranavir was again identified as a top hit and resulted in an IC_{50} value of 24.9 ± 9.8µM for Mrp3 mediated transport of CDF. If we compare these Mrp3 data with the better known and investigated rat and human MRP2 transporter isoforms, we can conclude that there is overlap in inhibitory potential since e.g. benzbromarone and tipranavir are also known inhibitors of Mrp2/MRP2 (Gilibili et al., 2017; Holmstock et al., 2018). These confirmed hits can be used as diagnostic inhibitors later on to investigate Mrp3 mediated efflux of potential compounds. The outcome of these Mrp3 mediated DDI investigations could then subsequently be implemented into physiologically based pharmacokinetic (PBPK) models to predict exposure to these substrate compounds *in vivo*. Another advantage of adding *in silico* investigation is the decreased number of experiments needed and thereby the decreased use of animals, so the 3R principle (replacement, reduction and refinement) can be applied to enhance animal welfare in the future.

In conclusion, 59 compounds were identified as Mrp3 inhibitors based on *in vitro* evaluation of more than 1500 compounds in suspended rat hepatocytes. Together with the *in vitro* screening, a naive Bayesian Mrp3 model was developed. Key physicochemical and structural features of Mrp3 inhibitors and non-inhibitors were elucidated and the final naive Bayesian model can be applied as a useful *in silico* screening tool to identify inhibitors of the Mrp3 transporter or to identify drug candidates that are likely to inhibit this membrane protein. Also, a 75% resemblance of hits was seen when Mrp3 transfected inside out membrane vesicles where used. Tipranavir was identified as one of the most potent Mrp3 inhibitors using these both approaches. The applied screening approaches of this work represent a first step in the future identification of novel and potent MRP3 inhibitors using human hepatocytes, although species differences have to be accounted for and the correct choice of substrate and *in vitro* model will be important to generate solid data.

Acknowledgements

We would like to thank Hermien Delanote and Bram Van Horenbeek for their technical contributions in the screening of novel Mrp3 inhibitors as part of their master theses. We would also like to thank Tom De Bruyn (Genentech) for his valuable comments on the prefinal manuscript.

Authorship contributions

Participated in research design: De Vocht, Hoeben, and Annaert.

Conducted experiments: De Vocht, Deferm, and Qi.

Performed data analysis: De Vocht, Buyck, and Annaert.

Wrote or contributed to the writing of the manuscript: De Vocht, Buyck, Deferm, Qi, Van Brantegem, van Vlijmen, Snoeys, Hoeben, Vermeulen and Annaert.

References

Ali, I., Welch, M.A., Lu, Y., Swaan, P.W., Brouwer, K.L.R., 2017. Identification of novel MRP3 inhibitors based on computational models and validation using an in vitro membrane vesicle assay. Eur. J. Pharm. Sci. Off. J. Eur. Fed. Pharm. Sci. 103, 52–59. https://doi.org/10.1016/j.ejps.2017.02.011

Annaert, P.P., Turncliff, R.Z., Booth, C.L., Thakker, D.R., Brouwer, K.L., 2001. P-glycoprotein-mediated in vitro biliary excretion in sandwich-cultured rat hepatocytes. Drug Metab. Dispos. Biol. Fate Chem. 29, 1277–1283.

Bow, D.A.J., Perry, J.L., Miller, D.S., Pritchard, J.B., Brouwer, K.L.R., 2008. Localization of P-gp (Abcb1) and Mrp2 (Abcc2) in Freshly Isolated Rat Hepatocytes. Drug Metab. Dispos. 36, 198–202. https://doi.org/10.1124/dmd.107.018200

Brouwer, K.L.R., Keppler, D., Hoffmaster, K.A., Bow, D. a. J., Cheng, Y., Lai, Y., Palm, J.E., Stieger, B., Evers, R., International Transporter Consortium, 2013. In vitro methods to support transporter evaluation in drug discovery and development. Clin. Pharmacol. Ther. 94, 95–112. https://doi.org/10.1038/clpt.2013.81

Chen, H.-L., Chen, H.-L., Liu, Y.-J., Feng, C.-H., Wu, C.-Y., Shyu, M.-K., Yuan, R.-H., Chang, M.-H., 2005. Developmental expression of canalicular transporter genes in human liver. J. Hepatol. 43, 472–477. https://doi.org/10.1016/j.jhep.2005.02.030

De Bruyn, T., van Westen, G.J.P., Ijzerman, A.P., Stieger, B., de Witte, P., Augustijns, P.F., Annaert, P.P., 2013. Structure-based identification of OATP1B1/3 inhibitors. Mol. Pharmacol. 83, 1257–1267. https://doi.org/10.1124/mol.112.084152

De Bruyn, T., Ye, Z.-W., Peeters, A., Sahi, J., Baes, M., Augustijns, P.F., Annaert, P.P., 2011. Determination of OATP-, NTCP- and OCT-mediated substrate uptake activities in individual and pooled batches of cryopreserved human hepatocytes. Eur. J. Pharm. Sci. Off. J. Eur. Fed. Pharm. Sci. 43, 297–307. https://doi.org/10.1016/j.ejps.2011.05.002

Deferm N, De Vocht T, Qi B, et al. Current insights in the complexities underlying drug-induced cholestasis. Crit Rev Toxicol. 2019;49(6):520-548. doi:10.1080/10408444.2019.1635081

Ellis, L.C.J., Grant, M.H., Hawksworth, G.M., Weaver, R.J., 2014. Quantification of biliary excretion and sinusoidal excretion of 5(6)-carboxy-2’,7’-dichlorofluorescein (CDF) in cultured hepatocytes isolated from Sprague Dawley, Wistar and Mrp2-deficient Wistar (TR(-)) rats. Toxicol. Vitro Int. J. Publ. Assoc. BIBRA 28, 1165–1175. https://doi.org/10.1016/j.tiv.2014.05.010

Fardel, O., Le Vee, M., Jouan, E., Denizot, C., Parmentier, Y., 2015. Nature and uses of fluorescent dyes for drug transporter studies. Expert Opin. Drug Metab. Toxicol. 11, 1233–1251. https://doi.org/10.1517/17425255.2015.1053462

Fukuda, Y., Takenaka, K., Sparreboom, A., Cheepala, S.B., Wu, C.-P., Ekins, S., Ambudkar, S.V., Schuetz, J.D., 2013. Human immunodeficiency virus protease inhibitors interact with ATP binding cassette transporter 4/multidrug resistance protein 4: a basis for unanticipated enhanced cytotoxicity. Mol. Pharmacol. 84, 361–371. https://doi.org/10.1124/mol.113.086967

Gilibili, R.R., Chatterjee, S., Bagul, P., Mosure, K.W., Murali, B.V., Mariappan, T.T., Mandlekar, S., Lai, Y., 2017. Coproporphyrin-I: A Fluorescent, Endogenous Optimal Probe Substrate for ABCC2 (MRP2) Suitable for Vesicle-Based MRP2 Inhibition Assay. Drug Metab. Dispos. Biol. Fate Chem. 45, 604–611. https://doi.org/10.1124/dmd.116.074740

Heredi-Szabo, K., Kis, E., Molnar, E., Gyorfi, A., Krajcsi, P., 2008. Characterization of 5(6)-carboxy-2,’7’-dichlorofluorescein transport by MRP2 and utilization of this substrate as a fluorescent surrogate for LTC4. J. Biomol. Screen. 13, 295–301. https://doi.org/10.1177/1087057108316702

Hirohashi, T., Suzuki, H., Takikawa, H., Sugiyama, Y., 2000. ATP-dependent Transport of Bile Salts by Rat Multidrug Resistance-associated Protein 3 (Mrp3). J. Biol. Chem. 275, 2905–2910. https://doi.org/10.1074/jbc.275.4.2905

Holmstock, N., Oorts, M., Snoeys, J., Annaert, P., 2018. MRP2 Inhibition by HIV Protease Inhibitors in Rat and Human Hepatocytes: A Quantitative Confocal Microscopy Study. Drug Metab. Dispos. Biol. Fate Chem. 46, 697–703. https://doi.org/10.1124/dmd.117.079467

International Transporter Consortium, Giacomini, K.M., Huang, S.-M., Tweedie, D.J., Benet, L.Z., Brouwer, K.L.R., Chu, X., Dahlin, A., Evers, R., Fischer, V., Hillgren, K.M., Hoffmaster, K.A., Ishikawa, T., Keppler, D., Kim, R.B., Lee, C.A., Niemi, M., Polli, J.W., Sugiyama, Y., Swaan, P.W., Ware, J.A., Wright, S.H., Yee, S.W., Zamek-Gliszczynski, M.J., Zhang, L., 2010. Membrane transporters in drug development. Nat. Rev. Drug Discov. 9, 215–236. https://doi.org/10.1038/nrd3028

Jemnitz, K., Heredi-Szabo, K., Janossy, J., Ioja, E., Vereczkey, L., Krajcsi, P., 2010. ABCC2/Abcc2: a multispecific transporter with dominant excretory functions. Drug Metab. Rev. 42, 402–436. https://doi.org/10.3109/03602530903491741

Kalliokoski, A., Niemi, M., 2009. Impact of OATP transporters on pharmacokinetics. Br. J. Pharmacol. 158, 693–705. https://doi.org/10.1111/j.1476-5381.2009.00430.x

Kawase, A., Yamamoto, T., Egashira, S., Iwaki, M., 2016. Stereoselective Inhibition of Methotrexate Excretion by Glucuronides of Nonsteroidal Anti-inflammatory Drugs via Multidrug Resistance Proteins 2 and 4. J. Pharmacol. Exp. Ther. 356, 366–374. https://doi.org/10.1124/jpet.115.229104

Keemink, J., Wuyts, B., Nicolaï, J., Jonghe, S.D., Stella, A., Herdewijn, P., Augustijns, P., Annaert, P., 2015. In vitro disposition profiling of heterocyclic compounds. Int. J. Pharm. 491, 78–90. https://doi.org/10.1016/j.ijpharm.2015.05.080

Kiuchi, Y., Suzuki, H., Hirohashi, T., Tyson, C.A., Sugiyama, Y., 1998. cDNA cloning and inducible expression of human multidrug resistance associated protein 3 (MRP3). FEBS Lett. 433, 149–152.

Köck, K., Brouwer, K.L.R., 2012. A Perspective on Efflux Transport Proteins in the Liver. Clin. Pharmacol. Ther. 92, 599–612. https://doi.org/10.1038/clpt.2012.79

Kool, M., van der Linden, M., de Haas, M., Scheffer, G.L., de Vree, J.M.L., Smith, A.J., Jansen, G., Peters, G.J., Ponne, N., Scheper, R.J., Elferink, R.P.J.O., Baas, F., Borst, P., 1999. MRP3, an organic anion transporter able to transport anti-cancer drugs. Proc. Natl. Acad. Sci. U. S. A. 96, 6914–6919.

Maeda, K., 2015. Organic anion transporting polypeptide (OATP)1B1 and OATP1B3 as important regulators of the pharmacokinetics of substrate drugs. Biol. Pharm. Bull. 38, 155–168. https://doi.org/10.1248/bpb.b14-00767

Matsushima, S., Maeda, K., Hayashi, H., Debori, Y., Schinkel, A.H., Schuetz, J.D., Kusuhara, H., Sugiyama, Y., 2008. Involvement of multiple efflux transporters in hepatic disposition of fexofenadine. Mol. Pharmacol. 73, 1474–1483. https://doi.org/10.1124/mol.107.041459

Nicolaï, J., 2015. Transport-metabolism interplay of atazanavir in rat hepatocytes (submitted).

Nicolaï, J., Thevelin, L., Bing, Q., Stieger, B., Chanteux, H., Augustijns, P., Annaert, P., 2017. Role of the OATP Transporter Family and a Benzbromarone-SensitiveEfflux Transporter in the Hepatocellular Disposition of Vincristine. Pharm. Res. 34, 2336–2348. https://doi.org/10.1007/s11095-017-2241-0

Nigam, S.K., 2015. What do drug transporters really do? Nat. Rev. Drug Discov. 14, 29–44. https://doi.org/10.1038/nrd4461

Parvez, M.M., Jung, J.A., Shin, H.J., Kim, D.H., Shin, J.-G., 2016. Characterization of 22 Antituberculosis Drugs for Inhibitory Interaction Potential on Organic Anionic Transporter Polypeptide (OATP)-Mediated Uptake. Antimicrob. Agents Chemother. 60, 3096–3105. https://doi.org/10.1128/AAC.02765-15

Rodrigues, A.D., Lai, Y., Cvijic, M.E., Elkin, L.L., Zvyaga, T., Soars, M.G., 2014. Drug-Induced Perturbations of the Bile Acid Pool, Cholestasis, and Hepatotoxicity: Mechanistic Considerations beyond the Direct Inhibition of the Bile Salt Export Pump. Drug Metab. Dispos. 42, 566–574. https://doi.org/10.1124/dmd.113.054205
Scialis, R.J., Csanaky, I.L., Goedken, M.J., Manautou, J.E., 2015. Multidrug Resistance-Associated Protein 3 Plays an Important Role in Protection against Acute Toxicity of Diclofenac. Drug Metab. Dispos. 43, 944–950. https://doi.org/10.1124/dmd.114.061705
Seelheim, P., Wüllner, A., Galla, H.-J., 2013. Substrate translocation and stimulated ATP hydrolysis of human ABC transporter MRP3 show positive cooperativity and are half-coupled. Biophys. Chem. 171, 31–37. https://doi.org/10.1016/j.bpc.2012.10.001
Sekine, S., Ito, K., Saeki, J., Horie, T., 2011. Interaction of Mrp2 with radixin causes reversible canalicular Mrp2 localization induced by intracellular redox status. Biochim. Biophys. Acta BBA - Mol. Basis Dis. 1812, 1427–1434. https://doi.org/10.1016/j.bbadis.2011.07.015
Shao, J., Markowitz, J.S., Bei, D., An, G., 2014. Enzyme- and transporter-mediated drug interactions with small molecule tyrosine kinase inhibitors. J. Pharm. Sci. 103, 3810–3833. https://doi.org/10.1002/jps.24113
Weininger, D., 1988. SMILES, a chemical language and information system. 1. Introduction to methodology and encoding rules. J. Chem. Inf. Comput. Sci. 28, 31–36. https://doi.org/10.1021/ci00057a005
Zamek-Gliszczynski, M.J., Xiong, H., Patel, N.J., Turncliff, R.Z., Pollack, G.M., Brouwer, K.L.R., 2003. Pharmacokinetics of 5 (and 6)-carboxy-2',7'-dichlorofluorescein and its diacetate promoiety in the liver. J. Pharmacol. Exp. Ther. 304, 801–809. https://doi.org/10.1124/jpet.102.044107
Zhang, Y.-K., Wang, Y.-J., Gupta, P., Chen, Z.-S., 2015. Multidrug Resistance Proteins (MRPs) and Cancer Therapy. AAPS J. 17, 802–812. https://doi.org/10.1208/s12248-015-9757-1
Zhu, Q.-N., Hou, W.-Y., Xu, S.-F., Lu, Y.-F., Liu, J., 2017. Ontogeny, aging, and gender-related changes in hepatic multidrug resistant protein genes in rats. Life Sci. 170, 108–114. https://doi.org/10.1016/j.lfs.2016.11.022

Footnotes

This research was supported by a research grant from the agency for Innovation by Science and Technology, Belgium (N° IWT150724).

Figure legends

Figure 1:

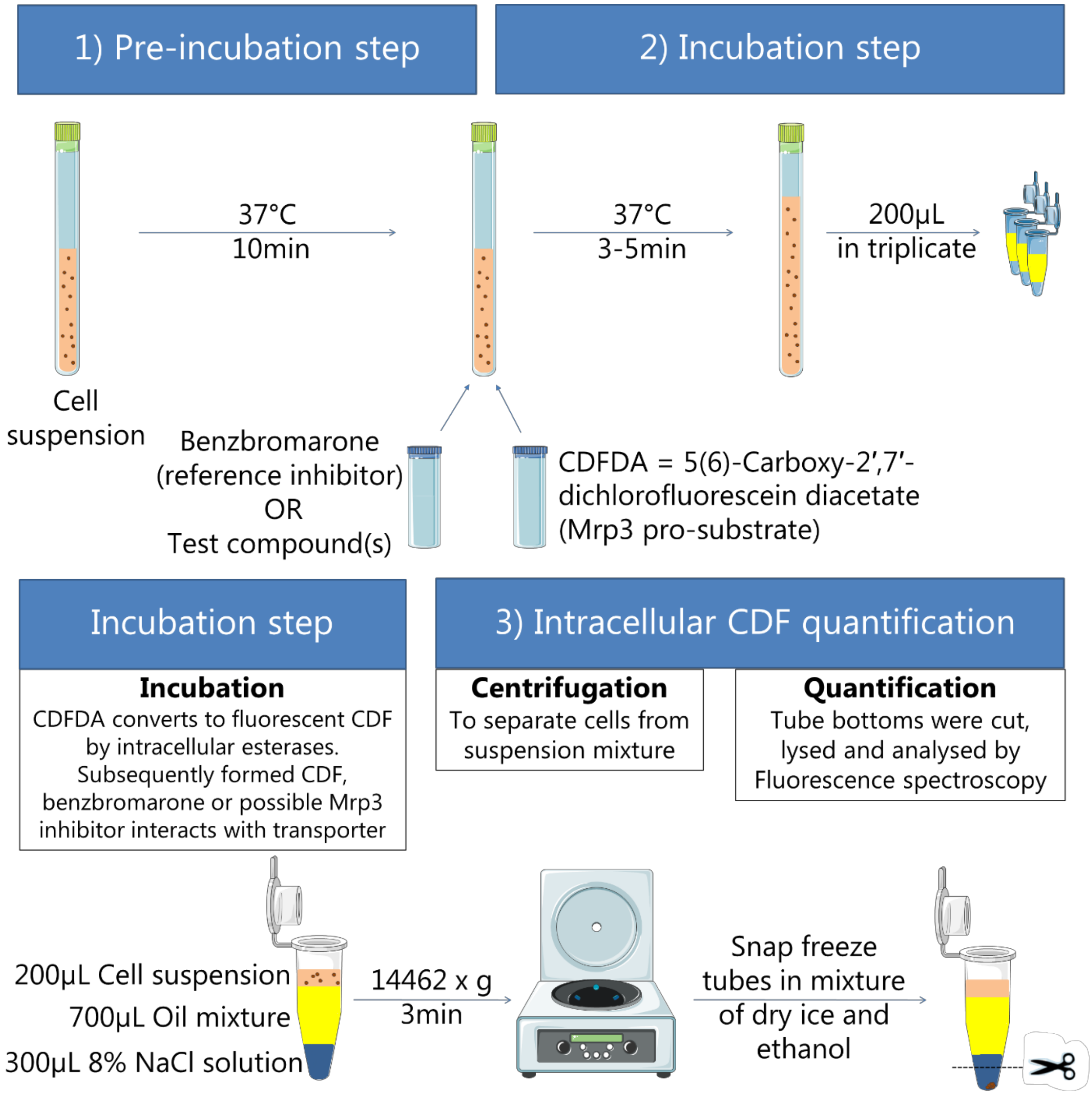

Figure 1: Graphical presentation of the optimized oil-spin assay used to screen Mrp3 inhibitors in rat hepatocytes in suspension.

Figure 2:

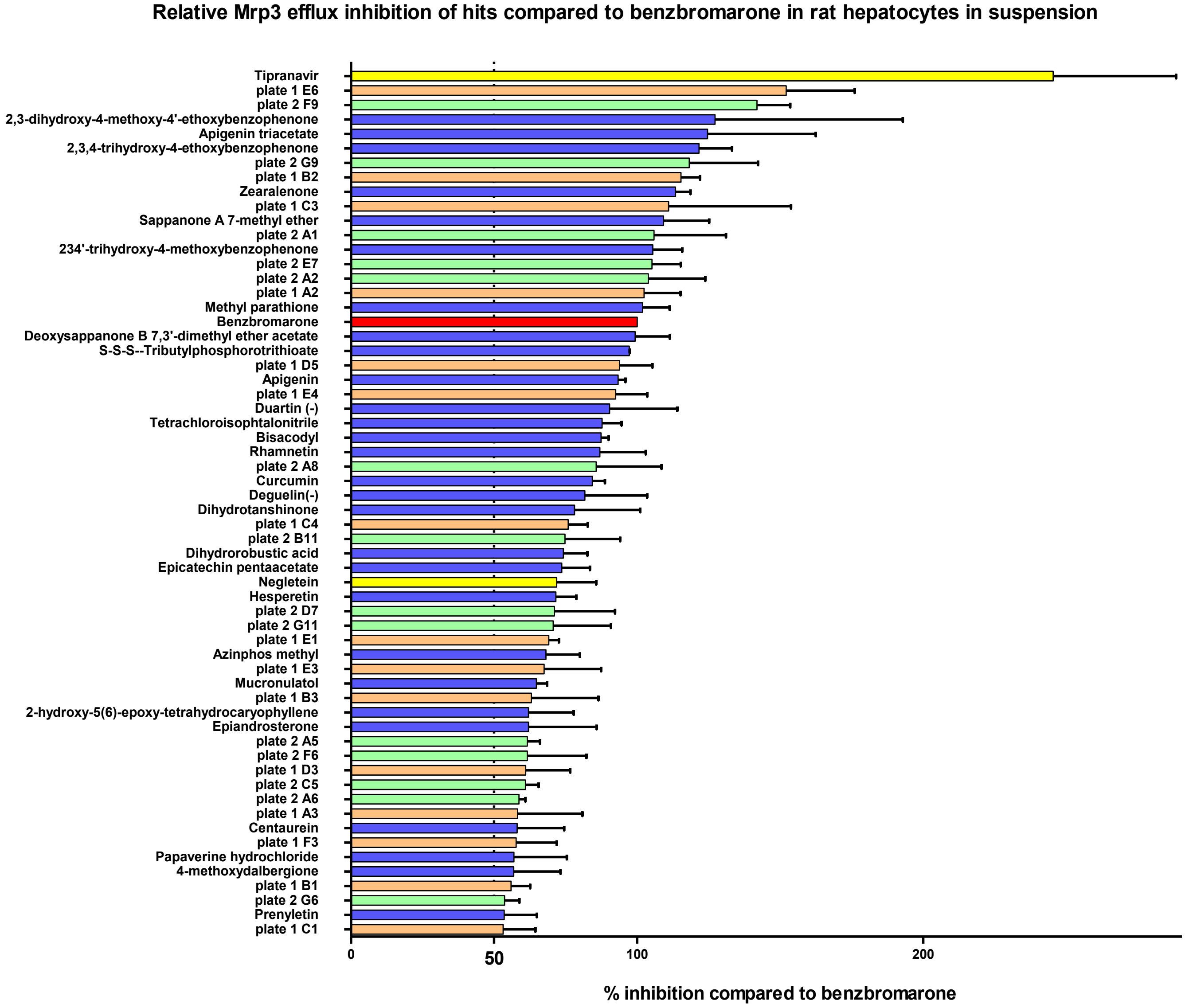

Color	Compound library	Hit rate	Screening
Blue	The Spectrum Collection	30/1444 (2.1%)	1
Yellow	In-house compounds		
Orange	First selection from Janssen corporate compound collection	15/50 (30%)	2
Green	Second selection from Janssen corporate compound collection	14/90 (15.6%)	3

Figure 2: A) Overview of all compounds (15µM) showing at least 50% inhibition compared to benzbromarone (5µM). Based on 3 and 5 min intracellular CDF levels, mean AUC (±SEM) values (n=3) were calculated and expressed as percentage of the AUC difference obtained for benzbromarone (100%) (red). A 50% cut-off was chosen to distinguish between non-inhibitors and inhibitors. After screening 1444 compounds of The Spectrum Collection library and in-house compounds (Screening 1), a hit rate of 2.1% (30 compounds - blue and yellow) was observed and a naive Bayesian model was constructed in Pipeline Pilot. Fifty compounds were selected from the Janssen corporate compound collection based on their chemical structures as being possible Mrp3 inhibitors as derived from this exploratory model. This second screening resulted in a hit rate of 30% (15 compounds; orange). A third screening of 90 compounds resulted in a hit rate of 16% (14 compounds; green). The overall hit rate was 3.7%, 59 hits out of 1584 compounds.

B) Overview of the several screening rounds and the respective hit rates.

Figure 3:

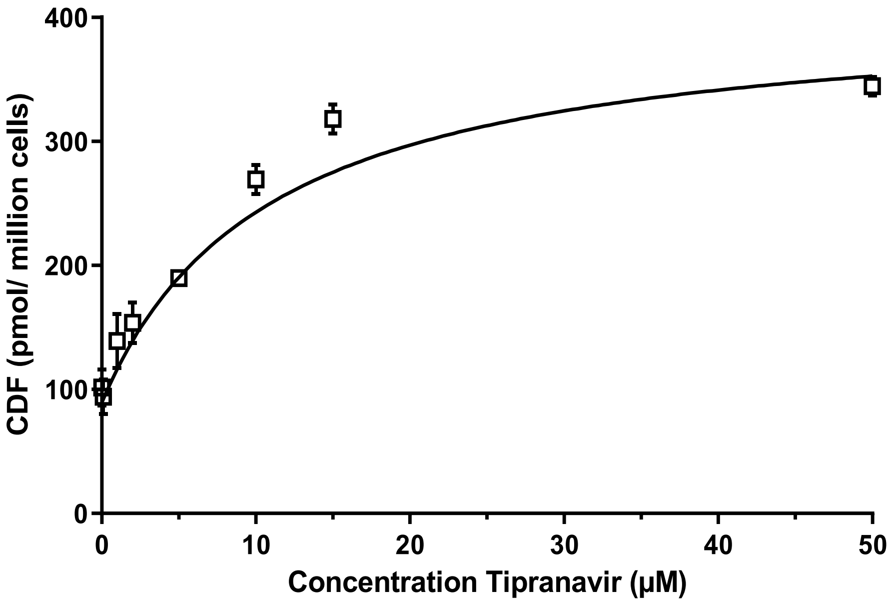

Figure 3: Inhibitory potency of tipranavir on Mrp3-mediated CDF transport. The IC_{50} value of tipranavir for Mrp3-mediated CDF transport (5 μM, 3 min incubation) was determined based on concentrations ranging from 0.1 to 50 μM. Values are expressed as intracellular CDF in pmol/million cells. Each value represents the mean ± SEM, n = 3. The IC_{50} value (mean ± SEM, n = 3 in triplicate) was calculated using non-linear least square regression for tipranavir (7.4 ± 2.1 μM).

Figure 4:

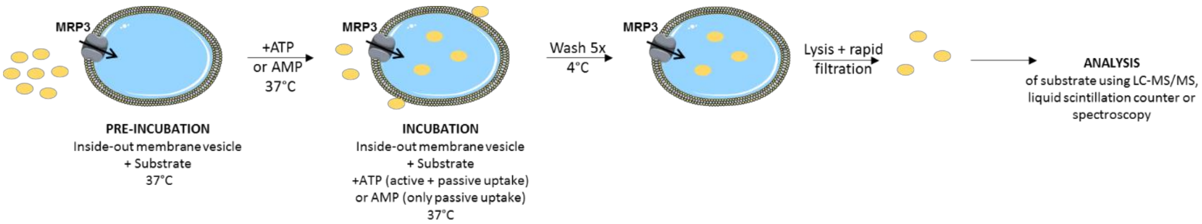

Figure 4: Graphical presentation of an optimized membrane vesicle assay used to screen Mrp3 inhibitors in Mrp3 transfected inside-out membrane vesicles.

Figure 5:

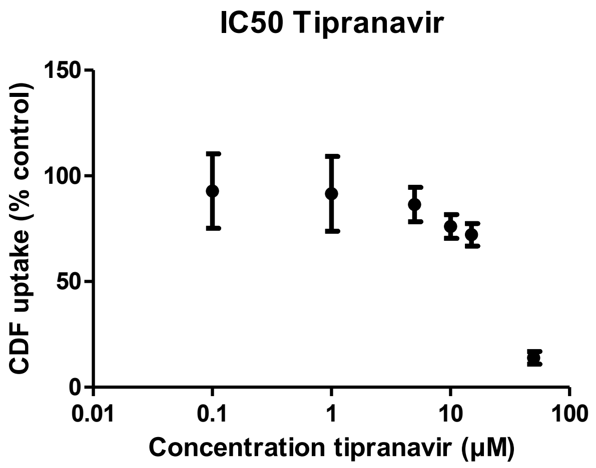

Figure 5: Inhibitory potency of tipranavir on Mrp3-mediated CDF transport using Mrp3 transfected inside-out membrane vesicles. The IC_{50} value of tipranavir for Mrp3-mediated CDF transport (5 µM, 30 min incubation) using the membrane vesicle assay was determined based on concentrations ranging from 0.1 to 50 µM. Values are expressed as % uptake of CDF compared to control without any modulator. Each value represents the mean ± SEM. The IC_{50} value (mean ± SEM, n = 3 in triplicate) was calculated using non-linear least square regression for tipranavir (24.9 ± 9.8µM).

Figure 6:

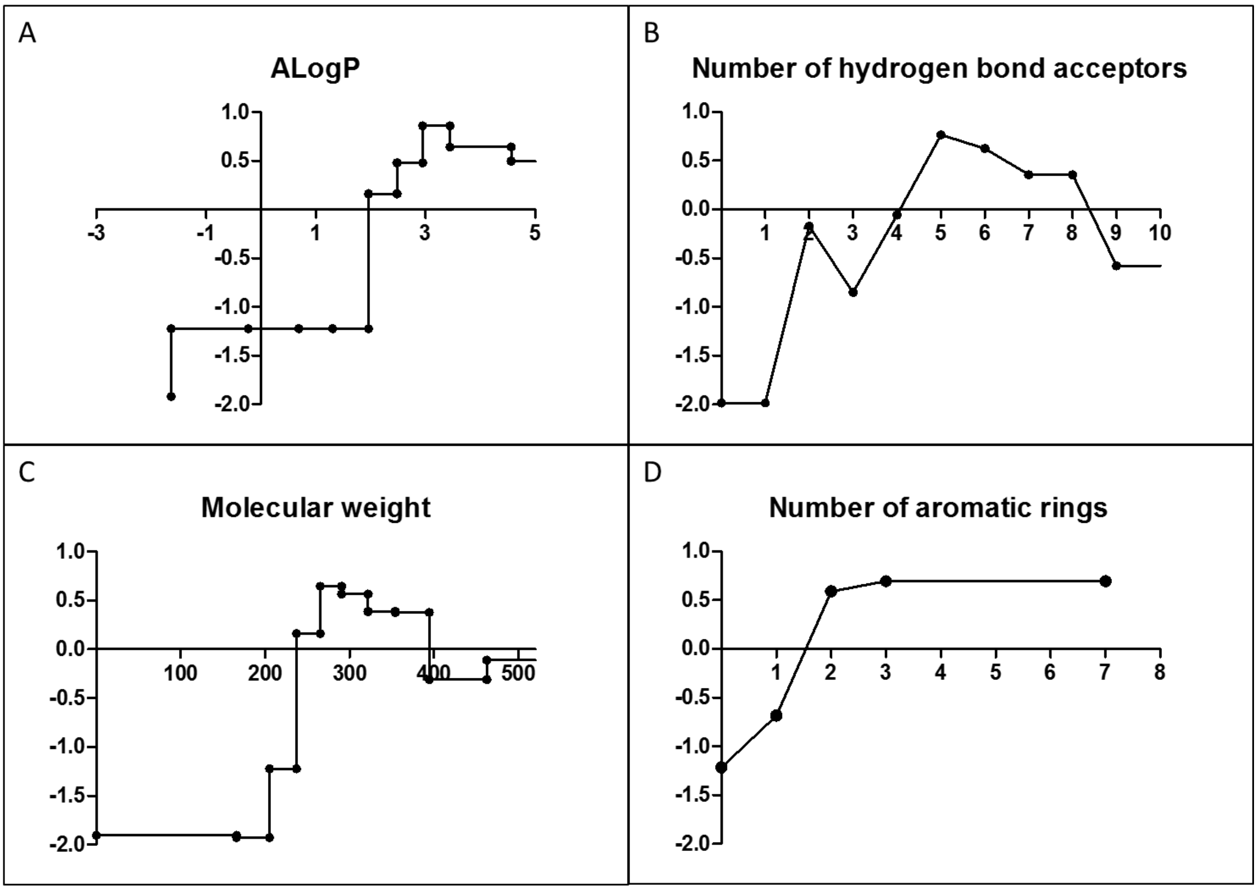

Figure 6: The 4 most pronounced physicochemical features to distinguish an Mrp3 inhibitor from a non-inhibitor include lipophilicity (A), number of hydrogen bond acceptors (B), molecular weight (C), and number of aromatic rings (D). The X-axis of each panel represents the respective physicochemical feature, while the Y-axis represents the normalized probability towards the 'good feature' (Mrp3 inhibitor) when > 0.05 and towards the 'bad feature' (Mrp3 non-inhibitor) when < -0.05.

Figure 7:

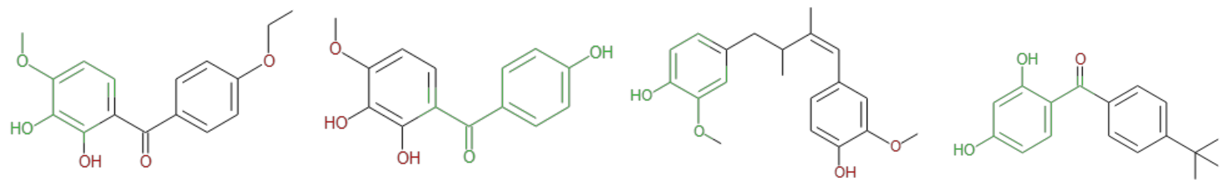

Figure 7: Example hit molecules with the green substructures representing ‘good’ sub-structural features with positive correlation with Mrp3 inhibition based on the Bayesian Mrp3 model.

Figure 8:

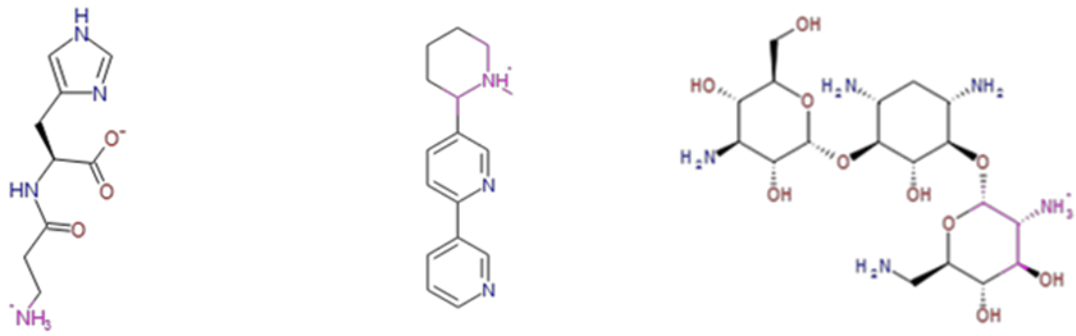

Figure 8: Example non-hit molecules with the pink substructures representing a ‘bad’ sub-structural feature with negative correlation with Mrp3 inhibition based on the Bayesian Mrp3 model.

Figure 9:

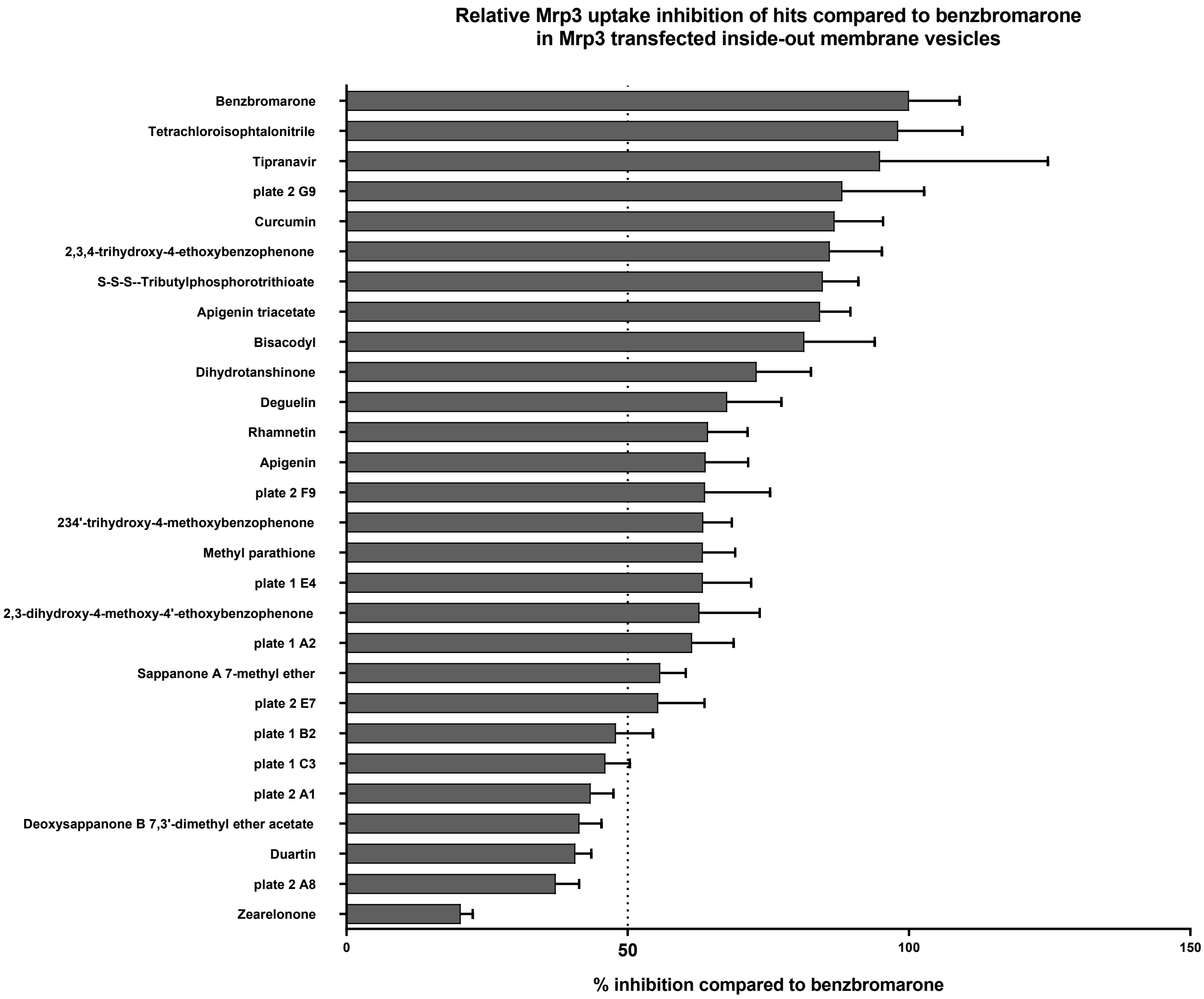

Figure 9: Overview of all compounds (50µM) tested using Mrp3 transfected inside-out membrane vesicle setup and ranked from high to low following their inhibitory potential compared to benzbromarone (50µM). The compounds showing at least 50% inhibition are ranked above of the 50% cut-off interval. Based on 30 min intracellular CDF levels (n=3), % inhibition compared to control ±SD were calculated and expressed.

Figure 10:

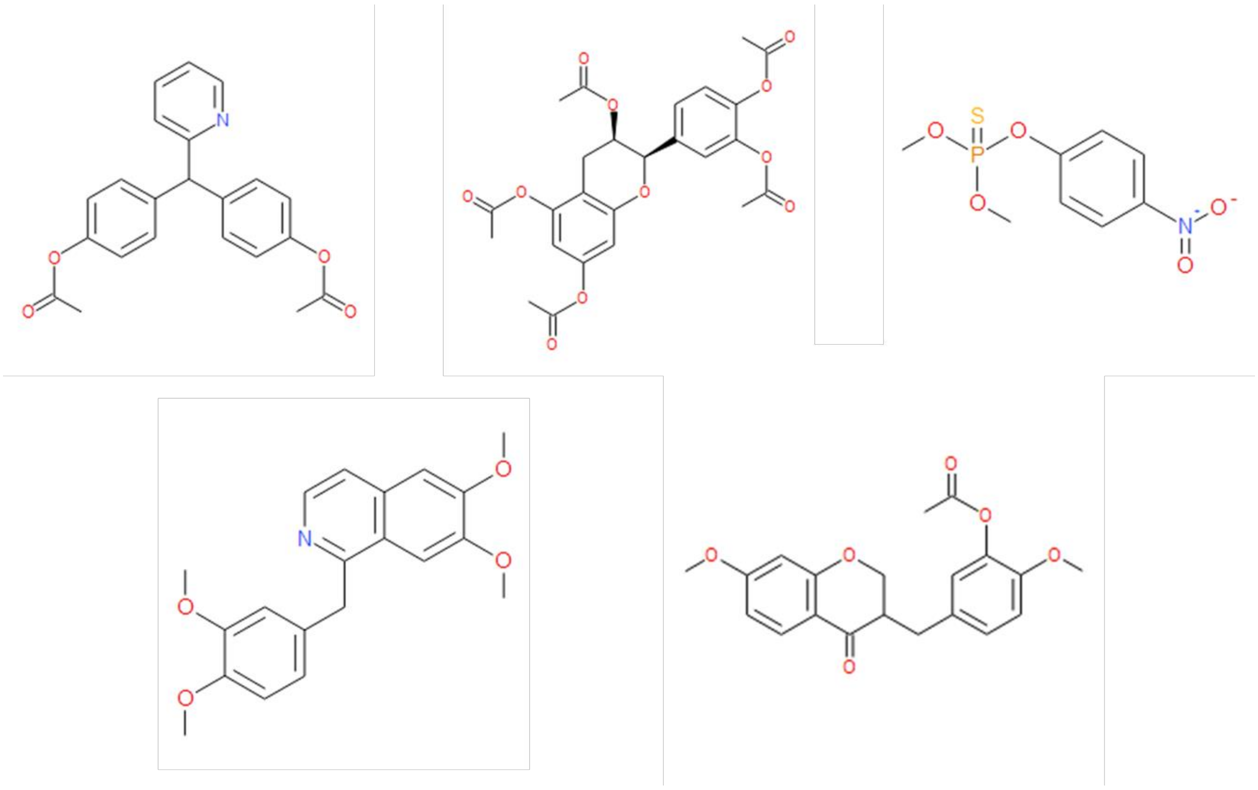

Figure 10: Example molecules that could potentially be metabolized to the corresponding phenolic acids.

Acknowledgements

We would like to thank Hermien Delanote and Bram Van Horenbeek for their technical contributions in the screening of novel Mrp3 inhibitors as part of their master theses. We would also like to thank Tom De Bruyn (Genentech) for his valuable comments on the prefinal manuscript.

Authorship contributions

Participated in research design: De Vocht, Hoeben, and Annaert.

Conducted experiments: De Vocht, Deferm, and Qi.

Performed data analysis: De Vocht, Buyck, and Annaert.

Wrote or contributed to the writing of the manuscript: De Vocht, Buyck, Deferm, Qi, Van Brantegem, van Vlijmen, Snoeys, Hoeben, Vermeulen and Annaert.